Status Report

For the period 6/1/91 through 5/31/92

On

Grant NAG 5-538

Studies of Regional and Global Tectonics and the Rotation of the Earth Using Very-Long-Baseline Interferometry

Prepared by J. X. Mitrovica and J. L. Davis

Irwin I. Shapiro
Principal Investigator

Harvard College Observatory
60 Garden Street
Cambridge, Massachusetts 02138

Reference: Grant NAG 5-538
Subject: Status Report for 6/1/91 through 5/31/92

Progress

Atmospheric gradient studies:

Work is continuing on the study of atmospheric gradients. We include a preprint outlining some recent results which have been submitted to the journal "Geophysical Research Letters".

Solid earth tides:

Work has begun on a study of solid Earth tidal deformations using the VLBI data set. At present we have examined deformations at the semi-diurnal tidal period using the IRIS data set. We presented preliminary results at the spring 1992 meeting of the American Geophysical Union in Montreal, Canada.

THE EFFECT OF TURBULENCE ON ATMOSPHERIC GRADIENT PARAMETERS DETERMINED FROM GROUND-BASED RADIOMETRIC AND SPACE GEODETIC MEASUREMENTS

James L. Davis
Harvard-Smithsonian Center for Astrophysics, Cambridge

Submitted to Geophysical Research Letters April 8, 1992

Abstract. Spatial and temporal fluctuations in the refractive index of air will effect estimates of atmospheric parameters determined from data obtained from radio signals which have propagated through the atmosphere. I present an expression for the covariance of a general vector of atmospheric parameters, and use this expression to calculate the effects on estimated gradient parameters of a frozen Kolmogorov turbulence field moving over a site at constant velocity. Numerical calculations are performed to investigate the implications for three techniques: ground-based microwave radiometry, and geodesy with the Global Positioning System and very long baseline interferometry. The results indicate that care must be taken in comparing gradient parameters determined using data from these different techniques.

1. Introduction

Atmospheric water vapor, located primarily in the lower troposphere, significantly effects the propagation of radio waves in this region by retarding and refracting them. The additive contribution of water vapor to the atmospheric refractive index is the wet refractivity. The wet refractivity varies spatially in an apparently random manner, with significant fluctuations occurring on a range of spatial scales, from microscopic scales (1 mm or less) to scales of several thousand kilometers. These fluctuations effect estimates of atmospheric parameters determined from observations sensitive to the atmospheric refractive index, such as ground-based remote microwave sensing of the atmosphere and space geodetic measurements. In particular, we will examine the effect of these fluctuations on the estimation of atmospheric-gradient parameters,

which have been investigated using both of these techniques [Davis et al., 1992; Rogers et al., 1992].

The development of a statistical model for gradient parameters will follow closely the methods and formalism of Treuhaft and Lanyi [1987] (hereafter referred to as TL). In particular, we will assume that the spatial fluctuations in the wet refractivity discussed above are described by Kolmogorov turbulence theory, and that temporal wet refractivity fluctuations are caused by the "frozen field" of spatial fluctuations borne horizontally by the wind. The assumption of Kolmogorov turbulence leads to the "2/3 law" for the structure function of wet refractivity fluctuations [Tatarskii, 1961]:

$$D_\chi(R) = \langle(\chi(\mathbf{r}+\mathbf{R}) - \chi(\mathbf{r}))^2\rangle = C^2 R^{2/3} \tag{1}$$

where $\mathbf{r}$ is a three-dimensional location vector, $\mathbf{R}$ a displacement vector (and R its length), χ the wet refractivity, and D_χ the structure function. The parameter C governs the power of the fluctuations. Like TL, we will assume that C does not vary spatially or temporally.

2. A Statistical Model for Estimated Parameters

In quantifying the effect of refractivity fluctuations on estimated gradient parameters, we must explicitly consider the method used to obtain the estimates. The

techniques mentioned above are not sensitive to fluctuations in the refractive index directly, but instead are sensitive to the wet delay, which is the integral of the refractivity along the line of sight:

$$\tau_{\epsilon,\theta,t} = \int_0^{h \csc \epsilon} ds\ \chi(\mathbf{r}(\epsilon,\theta,z),t) \tag{2}$$

where τ is the delay along the line-of-sight at time t in the direction of azimuth angle θ and elevation angle ϵ, and ds is the differential of distance along the line-of-sight path. In (2), we have parametrized the position vector $\mathbf{r}$ in terms of the elevation and azimuth angles, and the vertical coordinate z. The integral extends in height to h, the effective height of the troposphere, after the method of TL.

For an isotropic troposphere, the wet delay in (2) varies with elevation angle approximately as the cosecant of elevation angle. In order to compare propagation delays at different elevation angles, it is customary to use the "equivalent" zenith delay τ^z given by

$$\tau^z_{\epsilon,\theta,t} = \tau_{\epsilon,\theta,t} \sin\epsilon = \int_0^h dz\ \chi(\mathbf{r}(\epsilon,\theta,z),t) \tag{3}$$

In (3), even though the integration is performed in the zenith direction, the location vector $\mathbf{r}$ still varies along the true line of sight.

For ground-based microwave radiometry, the equivalent zenith delay forms our observable for the estimation of gradient parameters [Davis et al., 1992]. The entire set of observables can be represented by a vector $\mathbf{y}$, where

$$\mathbf{y}_i = \tau^z_{\epsilon_i,\theta_i,t_i} \tag{4}$$

and the estimated parameters $\mathbf{p}$, which include gradient parameters, can be estimated using the equation

$$\mathbf{p} = (A^T A)^{-1} A^T \mathbf{y} \tag{5}$$

where A is the so-called design or partial derivative matrix. The form (5) is simply the least-squares estimate of $\mathbf{p}$ assuming equal weight (i.e., equal variances) for the observations $\mathbf{y}$. Although in general we may not have equal weights, the assumption simplifies calculations without changing the conclusions of this study. Furthermore, we will assume for purposes of this study that the observations $\mathbf{y}$ are free from observational errors. This last assumption notwithstanding, the vector $\mathbf{p}$ is a random vector because the observations $\mathbf{y}$ are stochastic, as discussed above. Although Kolmogorov turbulence is in general nonstationary, during the period of observations we can define the average wet delay $\langle \mathbf{y} \rangle$, and the deviation from the average $\delta\mathbf{y} = \mathbf{y} - \langle \mathbf{y} \rangle$. The estimates of the parameters will then deviate from their "average" values by the amount

$$\delta\mathbf{p} = (A^T A)^{-1} A^T \delta\mathbf{y} \tag{6}$$

The expression (6) can be used to determine statistics for $\delta\mathbf{p}$. The expected value of this vector is just

$$\langle \delta\mathbf{p} \rangle = (A^T A)^{-1} A^T \langle \delta\mathbf{y} \rangle = 0 \tag{7}$$

Its covariance matrix is therefore

$$\langle \delta\mathbf{p} \delta\mathbf{p}^T \rangle = (A^T A)^{-1} A^T \langle \delta\mathbf{y} \delta\mathbf{y}^T \rangle A (A^T A)^{-1} \tag{8}$$

where we have used the fact that $(A^TA)^{-1}$ is symmetric. Denoting the covariance matrix of $\delta\mathbf{y}$ in (8) as T, the element T_{ij} is, using (2)–(4), given by

$$T_{ij} = \langle \delta\tau^z_{\epsilon_i,\theta_i,t_i} \delta\tau^z_{\epsilon_j,\theta_j,t_j} \rangle = \int_0^h dz \int_0^h dz' \ \langle \delta\chi(\mathbf{r}(\epsilon_i,\theta_i,z),t_i)\delta\chi(\mathbf{r}(\epsilon_j,\theta_j,z'),t_j)\rangle \quad (9)$$

where δ again denotes deviation from the average. The expectation in (9) is difficult to evaluate, because it involves refractivity separated not only in time but in space. However, using the frozen flow hypothesis discussed above, we have

$$\delta\chi(\mathbf{r}(\epsilon_j,\theta_j,z'),t_j) = \delta\chi(\mathbf{r}(\epsilon_j,\theta_j,z') - \mathbf{v}\Delta t_{ij}, t_i) \quad (10)$$

where $\Delta t_{ij} = t_j - t_i$ and $\mathbf{v}$ is the (horizontal) wind velocity vector, which we will take to be constant. Using (10), (9) can be written

$$\begin{aligned} T_{ij} &= \int_0^h dz \int_0^h dz' \ \langle \delta\chi(\mathbf{r}(\epsilon_i,\theta_i,z),t_i)\delta\chi(\mathbf{r}(\epsilon_j,\theta_j,z') - \mathbf{v}\Delta t_{ij}, t_i)\rangle \\ &= \int_0^h dz \int_0^h dz' \ \mathcal{R}_\chi(\mathbf{R}_{ij}) \end{aligned} \quad (11)$$

where $\mathcal{R}_\chi(\mathbf{R}_{ij})$ is the spatial covariance function for the wet refractivity fluctuations, evaluated at

$$\mathbf{R}_{ij} = \mathbf{r}(\epsilon_i,\theta_i,z) - \mathbf{r}(\epsilon_j,\theta_j,z') + \mathbf{v}\Delta t_{ij} \quad (12)$$

The covariance function can be written in terms of the structure function D_χ as

$$\mathcal{R}_\chi(\mathbf{R}) = \mathcal{R}_\chi(0) - \frac{1}{2}D_\chi(R) \quad (13)$$

The expression (11), along with the expression (1) for the structure function for Kolmogorov turbulence, enables us to evaluate the T_{ij} and hence the covariance matrix of estimated atmospheric parameters from (8).

3. Estimating Gradient Parameters: Numerical Results

We have undertaken to evaluate numerically (8) for the specific equivalent zenith delay model

$$\tau^z_{\epsilon,\theta,t} = \tau^z_o + V_z(t - t_o) + (G_n \cos\theta \cot + G_e \sin\theta) \cot\epsilon \tag{14}$$

The model (14) contains: a zenith delay parameter τ^z_o representing the zenith delay at the reference epoch t_o; zenith-delay rate parameter V_z; and two zenith-delay gradient parameters: G_n for the north direction and G_e for the east direction. (The azimuth angle is measured east from north.) The development of (14) is given in Davis et al. [1992].

To evaluate (8), we require a "schedule" of observations. We have chosen a schedule similar to that used by the WVR in the study in Davis et al. [1992]. This schedule, shown in Table 1, consists of a 360° azimuth scan at an elevation angle of 30°, followed by "tip" curves in the cardinal azimuths.

In performing the numerical integration, we expressed (11) using (13) and (1) as

$$\begin{aligned} T_{ij} &= \int_0^h dz \int_0^h dz'\ \mathcal{R}_\chi(\mathbf{R}_{ij}) \\ &= \int_0^h dz \int_0^h dz'\ \mathcal{R}_\chi(0) - \frac{1}{2}\int_0^h dz \int_0^h dz'\ D(R_{ij}) \\ &= \sigma^2_{\tau^z} - \frac{1}{2}C^2 \int_0^h dz \int_0^h dz'\ R^{2/3}_{ij} \end{aligned} \tag{15}$$

where we have used the fact that $\mathcal{R}_\chi(0)$ is the variance of refractivity fluctuations σ^2_χ, and we have expressed the quantity $h^2\sigma^2_\chi$ as $\sigma^2_{\tau^z}$, the variance of the zenith wet delay (see TL).

In performing the required integration numerically, we must specify the values of five quantities: (1) the zenith delay variance $\sigma^2_{\tau_z}$; (2) the strength parameter C; (3) the effective height of the troposphere h; (4) the wind speed v; and (5) the azimuth of the wind direction θ_v. For this study, we first adopted "standard" values for $\sigma^2_{\tau_z}$, C, and h (see Table 2), and performed the calculations for a range of wind speeds and azimuths. In the next section, we discuss the sensitivity of our results to changes those values.

The results of the calculations with the standard values are presented in Figure 1. This plot shows the standard deviation, i.e., the square root of the diagonal element of $\langle \delta \mathbf{p} \delta \mathbf{p}^T \rangle$ from (8), for the north gradient, G_n in (14), as a function of wind direction, for a range of wind velocities. The interpretation of this standard deviation is that, under the assumptions of Kolmogorov turbulence and the frozen flow model, and observations in directions and at times as shown by Table 1, and given the gradient model (14), if we have an ensemble of estimates of G_n, the standard deviations of those estimates will be as shown in Figure 1. (The expectation of the gradient estimates is zero.)

For the case $v = 0$ m s^{-1} Figure 1 indicates that there is no dependence on wind direction. For higher wind velocities, two major changes occur: the standard deviation of the gradient parameter decreases, and the variation with wind direction becomes more pronounced, with larger gradient estimates being more probable in directions orthogonal to the wind direction. This last result might seem counterintuitive, since one normally thinks of the wind as bringing in new air masses which may be more or less moist than the air mass currently over the site (as with the passage of a front).

Our model, however, did not include any real changes in atmospheric conditions, and Figure 1 represents the results for an atmosphere whose spatial variations are due solely to Kolmogorov-type (zero mean) turbulence. The explanation for the shape of the curves in Figure 1 lies instead with the effect of the wind velocity on the $\mathbf{R}_{ij}$ of (15). Referring to Figure 1, for a north-south wind, the $\mathbf{R}_{ij}$ oriented in an north-south direction are "longer," through (10), than those in the east-west direction, for equal elevation angles. In other words, the wind tends to effectively "compress" the field of fluctuations in the direction of the wind. The result of this compression is that the refractive index variations along the direction of the wind are averaged over a greater distance, with a greater probability of being averaged out. In this manner, a prevailing wind with no true static gradients may result in larger gradient estimates for the horizontal direction perpendicular to the wind than for that parallel to the wind, and may give the impression of a prevailing gradient.

This explanation also enables us to understand the asymmetries in Figure 1. This plot shows that the standard deviation for G_n for a wind blowing to the north is much smaller than that for a wind blowing to the south. This results from the particular observation schedule we chose, which starts with an observation in the north, and continues with observations at increasing azimuth angle. Thus, a wind directed towards the north blows the turbulence field away from the immediately subsequent observations, whereas a wind directed towards the south blows the turbulence field towards the immediately subsequent observations.

4. Sensitivity to Variations in Model Parameters

In the previous section, we presented our "standard" values for various parameters used in the numerical evaluation of $\langle \delta \mathbf{p} \delta \mathbf{p}^T \rangle$. It is straightforward to show that for the symmetric observing schedule of Table 1, the variance of the gradient estimates does not depend on our choice for $\sigma_{\tau_z}^2$. Figure 2 shows three curves. The solid line is our calculation using the standard values and for $v = 8$ m s^{-1}. The other curves represent values of C^2 and h increased by 50%. We can see that the size of the standard deviation of the estimate of G_n is sensitive to the values for these two quantities, but that our conclusions regarding the dependence on the wind azimuth are not. In both cases, the size of the gradients increase, for the same reason. In both cases the changes to the parameters cause an increase in the variance of the delay fluctuations, and larger gradient estimates can therefore be expected.

Figure 3 shows the results of our calculations for a change in the observing schedule. The elevation angle for the azimuth scan has been changed from 30° to 10°. In this case the gradient estimates will be much smaller, since, as with higher wind speed, the refractive index fluctuations will be averaged over much larger distances. For this wind speed, the direction of the wind has a much smaller effect since the large separation between the ray paths causes the correlation between observations to be small.

5. Ramifications for Microwave Radiometric and Space Geodetic Measurements

In the preceding sections, we calculated the effects on gradient parameters estimated from ground-based radiometric data of spatial fluctuations in the wet refractivity. We showed that a prevailing wind can lead to larger gradient estimates in some directions than in others, even when no prevailing gradients are present. The question arises as to whether our method for the analysis of the data was in some way faulty. In fact, our model for the equivalent zenith delay observations and our least squares inversion method did not take into account either of our basic assumptions concerning the structure of atmospheric turbulence and frozen flow. If these assumptions could be properly built into the analysis, no azimuthal variations should be apparent in Figure 1. These variations are thus understood to result from the limitations in our analysis model causing a coupling between the spatial/temporal correlations in the refractivity fluctuation field and the observing schedule.

For example, suppose that our data type were Global Positioning System (GPS) phase observations. GPS receivers are able to observe several satellites from different elevations and azimuths simultaneously. If we were to estimate atmospheric delay gradient parameters from each epoch of GPS observations, then it would be similar to our results in Table 1 for $v = 0$ m s^{-1}. Thus, there would be no preferred gradient direction for this single-epoch estimate. However, the correlation among atmospheric fluctuations effectively induces temporal and spatial correlations in the GPS observations, a case similar to that investigated for very long baseline interferometry (VLBI) by TL.

In the case of VLBI, observations are obtained at low elevation angles, often below 10°. In this case, the relevant curve is the $\epsilon = 10°$ in Figure 3. This shows that VLBI observations will also be less affected in the turbulence-only case by wind, and the estimated gradients will probably be much smaller than those estimated either from GPS or ground-based radiometric data. Rogers et al. [1992], who compare gradient parameters estimated from VLBI and radiometric data, seem to confirm this result, however the comparisons are made for different sites.

We have presented here results for an atmosphere which is unchanging except for (zero mean) fluctuations described by Kolmogorov turbulence. Clearly, there are instances where data clearly indicate the presence of a persistent azimuthal asymmetry [e.g., Dixon and Kornreich Wolf, 1990; Davis et al., 1992]. Such asymmetries may be caused by horizontal variations in humidity or temperature. The results in this paper describe expectations for estimated gradient parameters in the "background" case where no such horizontal variations exist.

Acknowledgements. I would like to thank J. Mitrovica for useful comments. This work was supported by NSF grant EAR-9105502, USGS grant 1434-92-G-2170, NASA grant NAG5-1930, and the Smithsonian Institution.

References

Davis, J.L., G. Elgered, A.E. Niell, C.E. Kuehn, Ground-based measurement of gradients in the "wet" radio refractive index of air, submitted to Radio Science, 1992.

Dixon, T.H., and S. Kornreich Wolf, Some tests of wet tropospheric calibration for the CASA Uno Global Positioning System experiment, Geophys. Res. Lett., 17, 203–206, 1990.

Rogers, A.E.E., and 34 others, Improvements in the accuracy of geodetic VLBI, submitted to AGU monograph on the NASA Crustal Dynamics Project, 1992.

Tatarskii, V.I., Wave Propagation in a Turbulent Medium, trans. R.A. Silverman, McGraw-Hill, New York, 1961.

Treuhaft, R.N. and G.E. Lanyi, The effect of the dynamic wet troposphere on radio interferometric measurements, Radio Science, 22, 251–256, 1987.

Table 1. Observation "schedule."

Azimuth (deg)	Elevation (deg)	Time (sec)
0	30	0
20	30	20
⋮	⋮	⋮
340	30	340
0	20	360
0	30	370
–	90	380
180	30	390
180	20	400
90	20	420
90	30	430
–	90	440
270	30	450
270	20	460

Table 2. Standard values for parameters.

Parameter†	Value
$\sigma_{r_z}^2$	5 mm
C	2.4×10^{-7} m$^{-1/3}$
h	1 km

†Standard values for C and h taken from Treuhaft and Lanyi [1987].

Figure Captions

Fig. 1. Standard deviation of the estimated north gradient parameter G_n as a function of wind direction, for various wind speeds. The observing schedule of Table 1 and the standard values for $\sigma_{\tau_x}^2$, C, and h from Table 2 were used. (a) $v = 0$ m s^{-1}. (b) $v = 2$ m s^{-1}. (c) $v = 4$ m s^{-1}. (d) $v = 6$ m s^{-1}. (e) $v = 8$ m s^{-1}. (f) $v = 10$ m s^{-1}.

Fig. 2. Standard deviation of the estimated north gradient parameter G_n as a function of wind direction, for a wind speed of 8 m s^{-1}. The observing schedule of Table 1 was used. (a) Standard values from Table 2. (b) $C^2 = 1.5\times$ standard value. (c) $h = 1.5\times$ standard value.

Fig. 3. Standard deviation of the estimated north gradient parameter G_n as a function of wind direction, for a wind speed of 8 m s^{-1}. The standard values from Table 2 were used. (a) Observing schedule from Table 1. (b) Observing schedule from Table 1, except the azimuth scan was performed at an elevation angle of 10°.

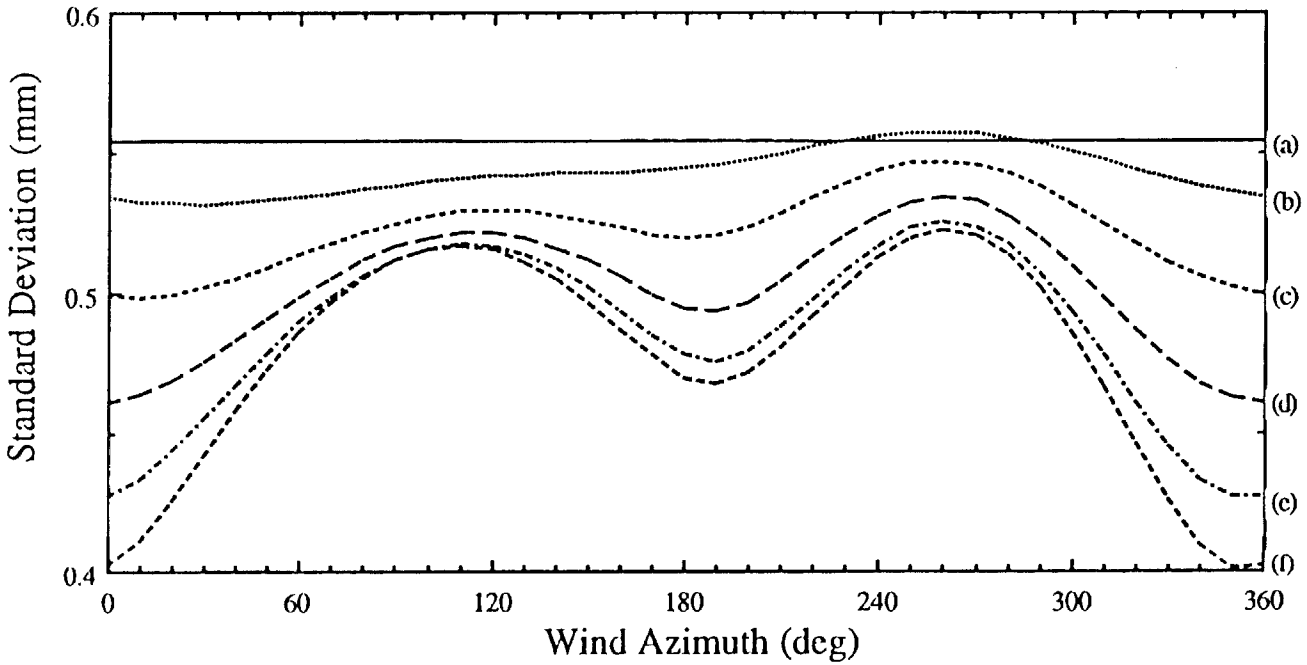
0.6
0.5
0.4
Standard Deviation (mm)
0
60
120
180
240
300
360
Wind Azimuth (deg)
(a)
(b)
(c)
(d)
(e)
(f)

Fig 1

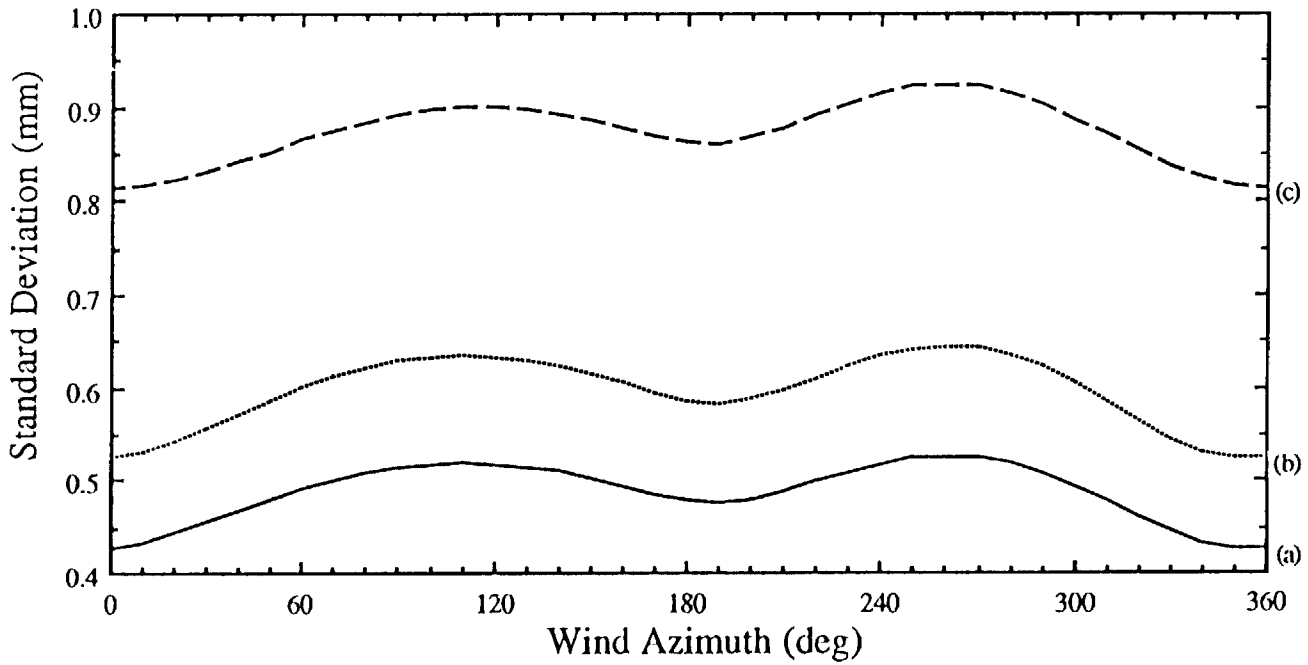
Standard Deviation (mm)
1.0
0.9
0.8
0.7
0.6
0.5
0.4
0
60
120
180
240
300
360
Wind Azimuth (deg)
(c)
(b)
(a)

Fig 2

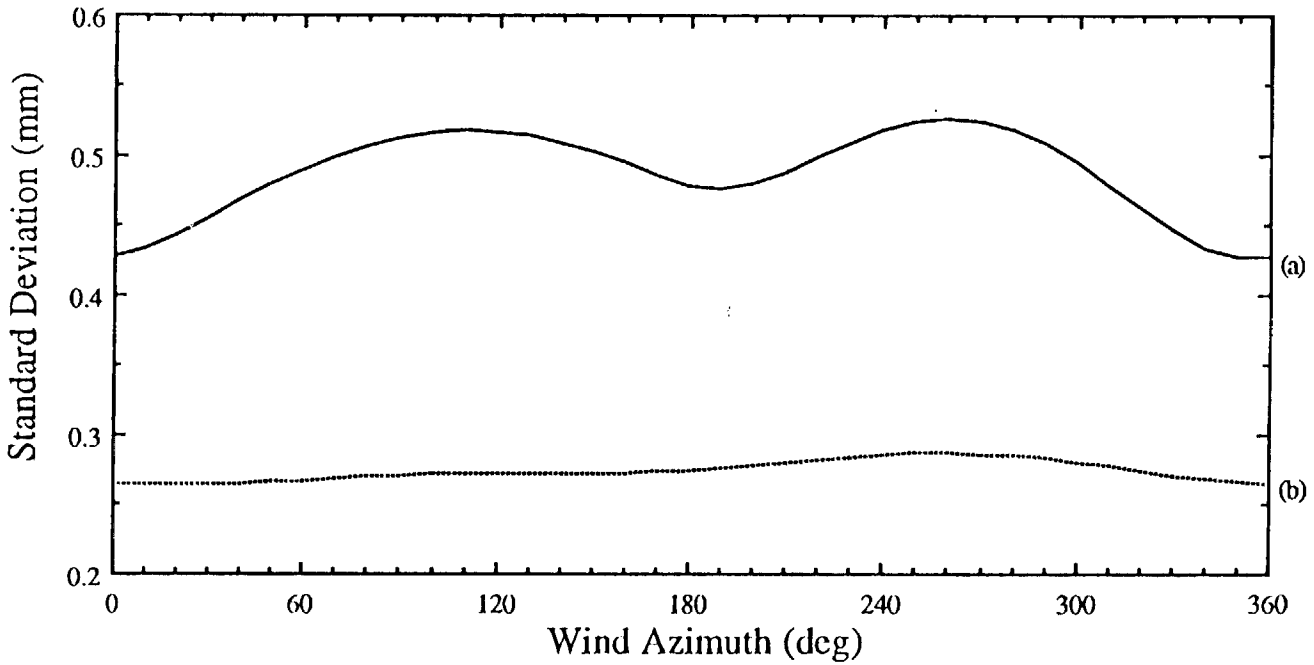
0.6
0.5
0.4
0.3
0.2
Standard Deviation (mm)
0
60
120
180
240
300
360
Wind Azimuth (deg)
(a)
(b)

Fig 3